



Development of intelligent system models for prediction of licorice concentration during nanofiltration/reverse osmosis process

Alireza Rayegan Shirazi Nejad^a, Abol Mohammad Ghaedi^{b,*}, S.S. Madaeni^c, M.M. Baneshi^a, Azam Vafaei^b, Daryoush Emadzadeh^{d,*}, W.J. Lau^e

^a*Social Determinants of Health Research Center, Yasuj University of Medical Sciences, Yasuj, Iran, email: alirezaraygan47@yahoo.com (A.R.S. Nejad), mmbaneshi@yahoo.com (M.M. Baneshi)*

^b*Department of Chemistry, Gachsaran Branch, Islamic Azad University, P.O. Box 75818-63876, Gachsaran, Iran, Tel. +98-7432332033, email: abm_ghaedi@yahoo.com (A.M. Ghaedi), a.vafaei11@yahoo.com (A. Vafaei)*

^c*Membrane Research Center, Chemical Engineering Department, Razi University, Kermanshah, Iran, email: smadaeni@yahoo.com (S.S. Madaeni)*

^d*Department of Chemical Engineering, Gachsaran Branch, Islamic Azad University, Gachsaran, Iran, email: d.emadzadeh@gmail.com (D. Emadzadeh)*

^e*Advanced Membrane Technology Research Centre, Universiti Teknologi Malaysia, 81310 Skudai, Johor, Malaysia, email: kwoeijye@utm.my (W.J. Lau)*

Received 27 May 2018; Accepted 29 December 2018

ABSTRACT

Reverse osmosis (RO) and nanofiltration (NF) membranes in spiral wound configurations have been widely used in food processing ranging from dairy to fruit juice for concentration, purification and recovering valuable components. In this work, intelligent systems, i.e., back-propagation artificial neural network (BPNN), radial basis function (RBF), fuzzy inference system (FIS) and adaptive Neuro-fuzzy inference system (ANFIS) were employed to predict the water flux and solute rejection of RO and NF membrane during concentration of licorice solution. To develop the intelligent systems, normalized membrane type, temperature, pressure, pH and cross-flow velocity are taken as inputs while normalized permeate flux and rejection are as outputs of the models. The proposed intelligent systems have been compared based on statistical parameters of the coefficient of determination (R^2) and the mean absolute error (MAE). The results indicate that the ANFIS model is more accurate and reliable compared to the BPNN, RBF and FIS approaches. It was found that the predictions using ANFIS model were usually in good agreement with the experimental data, showing the R^2 values within the range of 0.932–0.997 and the MAE values in the range of 0.01–1.7%. On the basis of comparison among the results obtained from this investigation, it is suggested that the ANFIS model could be potentially utilized to forecast the rejection and permeate flux of membrane during the concentration process of a licorice solution.

Keywords: NF and RO membranes; Backpropagation neural network (BPNN); Concentration; Fuzzy inference system (FIS); Radial basis function (RBF); Adaptive neuro-fuzzy inference system (ANFIS); Licorice solution

1. Introduction

Licorice (*Glycyrrhiza glabra* L.) is one of the most popular herbal plants in many countries such as Iran and China.

Triterpene glycosides and flavonoids are the main active ingredients of licorice. These compounds exhibit various types of pharmacological activity such as antimicrobial, anti-allergic, antihepatocarcinogenic, anti-inflammatory, antiatherogenic, etc. [1–5].

*Corresponding author.

Presented at the EDS conference on Desalination for the Environment: Clean Water and Energy, Rome, Italy, 22–26 May 2016.

The conventional concentration techniques - vacuum distillation and evaporation that are employed today have some disadvantages, including the use of high temperatures, toxic solvents and high energy consumption. Additionally, the heat treatment can alter the characteristics of compounds such as the flavour and sensory characteristics [6]. The use of membrane concentration techniques has become more and more important in the food and beverage industry due to unique advantages, namely low temperatures, lack of phase change and low energy consumption [7–9]. Concentration of licorice aqueous solutions by traditional evaporation processes is being replaced by nanofiltration (NF) and reverse osmosis (RO) based membrane processes [10]. However, the membrane technologies are unsuitable for the concentrations normally higher than 25–30° Brix. This is because when the juice concentration is increased significantly, the osmotic pressure becomes equal to the hydraulic pressure, causing no flux produced. Another key disadvantage of membrane technology is the fouling that causes a decline in flux and therefore a loss in process yield over time. It is necessary to mention that the key advantage of thermal evaporation is the concentration of the liquid food up to 65° Brix [11,12].

In general, the permeate flux and rejection are considered as the main indicators of membrane process performance which significantly affect the cost of treatment. In most of the cases, the membrane characteristics, fluid properties, physicochemical properties of solute and operation conditions are main factors determining flux and rejection. Therefore, the study of solute rejection and permeation flux are needed for the design and evaluation of a new membrane process for industrial scale separation [13,14]. There are various mathematical models to simulate mass transfer, flux decline and solute rejection of fruit juice and wastewater using membrane technologies [15–17]. Curcio et al. [18] for instance studied transport phenomena in membrane for the process of licorice solutions concentration. They used the numerical solution of partial differential equations by a finite element technique for the non-Newtonian behavior of licorice solutions. The proposed model correlates the influence of flow rate, concentration, membrane hydraulic permeability, fluid rheological and trans-membrane pressure on the permeate flux decline and solute rejection.

Each of conventional models (mathematical equations) based on physical concepts has its own limitations. Typically, the equations employed are often complex and need some experimental data to determine the system parameters. In addition, each equation is only valid for certain food process under specific operating conditions and most of these models are obtained by means of a steady state hypothesis. Because of this, the predictions of these models are not always satisfactory [19,20].

Intelligent system models such as artificial neural network (ANN), fuzzy logic (FL) and adaptive Neuro-fuzzy inference system (ANFIS) can be applied as an alternative to mathematical models for determining complex connections between many inputs and outputs [21–23]. Recently, artificial neural network has been utilized as a powerful modeling tool in membrane technology [24–26]. There are several researchers who studied the applicability of ANN and ANFIS to describe membrane filtration. Nandi et al. [14] used low cost ceramic microfiltration membrane in

the oily wastewater treatment. They developed an artificial neural network model and the cake filtration model to forecast permeate flux and concluded that the ANN model performs better than the cake filtration model for the prediction of permeate flux with lower error values.

Aydiner et al. [27] on the other hand investigated the ability of ANN and Koltuniewicz's method to model flux decline in crossflow microfiltration of a mixture containing phosphate and fly ash under various conditions, i.e., phosphate concentration, fly ash dosage, trans-membrane pressure and membrane type. The results of ANN models showed that they are able to simulate the decline of permeate flux at a high precision from experimental conditions. Yangali-Quintanilla et al. [28] applied ANN models based on the quantitative structure-activity relationship (QSAR) to forecast the rejection of natural organic compounds using polyamide RO and NF membranes. They defined the QSAR equation using principal component analysis and multiple linear regression as a function of solute properties, membrane characteristics and operating conditions. The results indicated that the predicted and experimental rejections could be modeled with good correlations.

Artificial neural network models have also been successfully applied to predict different aspects of membrane filtration. Some of the examples include simulating the batch ultrafiltration performance of mosambi juice and synthetic fruit juice [20], fouling of membrane during crossflow microfiltration [29], process optimization of seawater RO desalination plant [30], predicting NF membrane fouling [31], using electro dialysis for lead ions separation from wastewater [32] and prediction of microfiltration membrane fouling [33].

Fuzzy inference system (FIS) has been utilized to solve the nonlinearity problem. It is considered to have low mathematical equation requirements. FIS has been successfully applied to model membrane processes [34]. Madaeni and Kurdian [13] used hybrid genetic algorithm and fuzzy logic for modeling and virus removal optimization from water using dead-end microfiltration process. The parameters of flux and rejection were experimentally achieved under various conditions compared with those obtained through fuzzy logic. The results showed that fuzzy logic simulates flux and rejection within an acceptable error range. Rahmadian et al. [35] applied fuzzy logic for removal of lead ions from aqueous solutions by micellar-enhanced ultrafiltration. They claimed that the fuzzy logic model is simpler and easier than the mathematical modeling for the description of the relationships among the different conditions and the permeate flux and rejection. The results indicated that there is a very good agreement between the predicted values achieved from the fuzzy model and the actual data.

Adaptive neuro-fuzzy inference (ANFIS) that combines fuzzy logic and ANN is able to train from the data based on the characteristics of the input and output, and create membership functions and rules through learning from the data by the ANN. The accuracy of modeling using the fuzzy logic can be greatly enhanced [36,37]. Vural et al. [19] employed ANFIS to model performance of a proton exchange membrane fuel cell under different operating conditions. The results displayed very good agreement between the actual data and those forecasted by ANFIS model. Sargolzaei et al. [38] employed back propagation artificial neural network

(BPNN), radial basis function (RBF) and ANFIS to predict permeate flux and starch rejection from wastewater by a polyethersulfone membrane. Their results demonstrated that the ANFIS provides a better prediction than RBF and BPNN models.

In this work, intelligent systems (BPNN, RBF, FL and ANFIS) are utilized to model performance of cross-flow NF and RO process for concentrating licorice aqueous solutions and to predict permeate flux and rejection under various operating conditions.

2. Materials and methods

2.1. Experimental data

The experimental data which has been applied to train and test intelligent models, explanation of the schematic diagram and membrane specifications can be found in our previous research [10]. We performed different experimental trials with membranes having a surface area of 0.002 m². The cross-flow velocity, trans-membrane pressure, pH and temperature were varied during experiment in the range of 0.5–3.2 m/s, 6–14 bar, 3–11 and 25–45°C, respectively.

2.2. Theory of ANN

ANN is a simplified model of the human brain. The neural network can be used to model nonlinear systems by establishing the relation between input and output variables via a training data set. The following equation can be applied to the training process.

$$y_j = \sum_{k=1}^n w_{jk} x_k + b_j \quad (1)$$

where x_k shows the input, n is the input node number, w_{jk} is the weight from k th to j th neurons, and b_j is the j th neuron bias. The output y_j is attained via adjusting weights w_{jk} in the networks [33].

Connections among neurons for various layers and within layers are significant in the construction of a ANN. Feed forward neural network is the most common and most widely applied models among abundant practical applications [39,40]. After a neuron receives the input, it does its function and produces a single output transferring its output to all of the neurons. In the feed forward network, a linear or nonlinear transfer function sends the neuron outputs of the first layer to the neurons of the second layer. One of the pivotal factors which tally inputs with outputs in different ways is transfer function [20]. Three types of the most commonly applied transfer functions are the sigmoid, linear and hyperbolic tangent function. The transfer functions are as follows [32]:

Sigmoid transfer function

$$f(x) = \frac{1}{1 + e^{-x}}, 0 \leq f(x) \leq 1 \quad (2)$$

Linear transfer function

$$f(x) = x, -\infty \leq f(x) \leq +\infty \quad (3)$$

Hyperbolic transfer function

$$f(x) = \tanh(x) = \frac{e^x - e^{-x}}{e^x + e^{-x}}, -1 \leq f(x) \leq 1 \quad (4)$$

The selection of the number of hidden layers and the number of neurons per each hidden layer can change the complexity of the ANN model. The determination of the number of layers and neurons is complicated as they depend on certain problem and are performed through trial and error approach. With too few neurons, the ANN may not be able to figure out the problem and with a large number of neurons it may lead to overfitting [41,42]. Overfitting is one of the problems that taking place during neural network training. Even though the error on the training set is driven to a very small value, when new data are shown to the network the error is relatively large. The ANN has memorized the learning data set, but it has not trained to generalize to new observation and will not give precise predictions. Early stopping and regularization are two methods that used to avoid overfitting and raising generalization.

In early stopping methods the total data is split into three subsets: training, validation and testing subsets. Training set is used to determine weights and biases of network. During training process, the error on the validation set is recorded. The validation error ordinarily diminishes during the initial subset of training, as does the training set error. Nevertheless, the validation would usually start to increase when error the network begin to memorize the data. The train stops, and the weights and biases at the minimum of the validation error are relapsed when the validation error broaden for a specified number of repetition.

2.2.1. Training of ANN

The neural network toolbox in Matlab7(R2009a) was applied to simulate the experimental data. The total data were divided into three sets for modeling of flux and rejection. Both sets contain 34 data. Total 34 data of each set were split into three subsets. 70% of samples were applied to learning and 12% of data were employed to validation and 18% of data, which has not been employed in the training process, were utilized for generalization. Each data set consists of five inputs: type of membrane (RO and NF), trans-membrane pressure (bar), feed temperature (°C), cross flow velocity (m/s), and pH. The network outputs are permeate flux (L/m²·h) and rejection (%), respectively. Two different ANN architectures (BPNN and RBF structures) were established for simulation permeate flux and rejection during RO and NF of licorice aqueous solutions concentration.

2.2.2. BPNN architecture

A BPNN model with single and double hidden layer was employed. The trial and error method was used to appointed the hidden layers neurons. The optimal network architecture of a typical BPNN is shown in Fig. 1. The Levenburg-Marquardt (LM) method was applied as the back propagation algorithm to amend the learning rate and stability of the back propagation algorithm for seeking the minimum mean absolute errors (MAE) between experi-

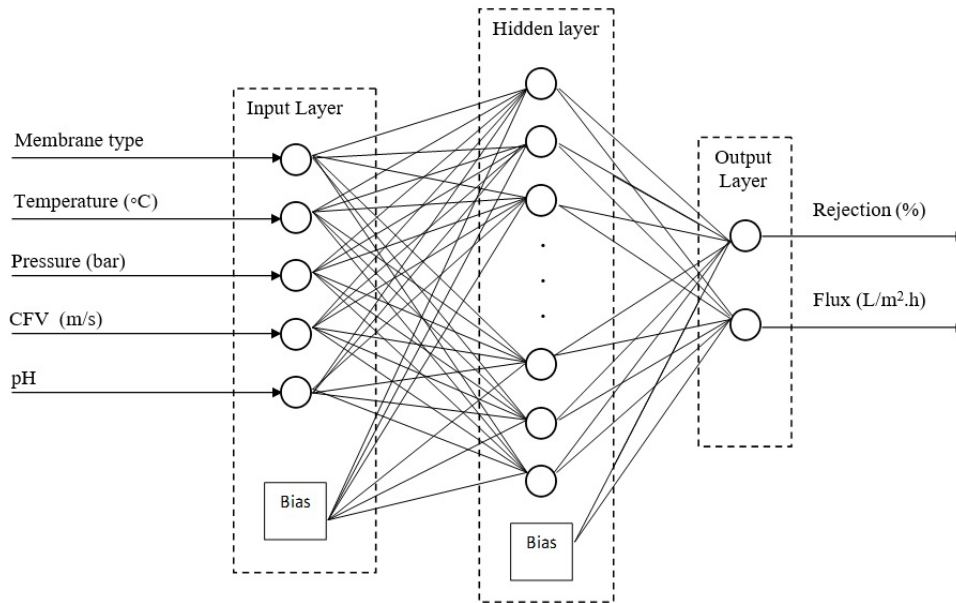


Fig. 1. A typical architecture of BPNN model.

mental data and predicted values. The change rate of connection weights during training is displayed by learning rate. The choice of a training rate is of essential importance to find the local minimum error [20]. In the present work, the learning rate of 0.2 was selected because a lower value enhances the convergence time and high oscillations in error were noticed at higher training rates. The weights for each input and iterations (10000) were randomly initialized. The BPNN applied in this work is based on the following equation:

$$y_k = F \left(\sum_m^{j=1} W_{jk} \times F \left(\sum_n^{i=1} W_{ij} X_i \right) \right) \quad (5)$$

where y_k is the output value, F is the transfer function, W_{jk} is the connection weight between the hidden layer and the output layer, W_{ij} is the connection weight between the input layer and the hidden layer and X_i is the input value of the network.

2.2.3. RBF architecture

Fig. 2 displays a schematic diagram for a radial basis function neural network (RBFNN). The RBFNN was presented by many researchers [22,23,43–45] and appears a better alternative to BPNN as RBFNN supplies easier initialization, faster learning procedure, and more stable performance [43]. The RBFNN has a feed forward architecture. However, the BPNN is one of the most widely applied ANN models in many research papers. The basic construction of an RBFNN normally is composed of three layers: (a) the input layer, (b) the hidden layer and (c) the output layer. RBFNN can prevail over some of the BPNN problems using the non-linearity in the transfer functions of the hidden layer neurons [46]. Diversity of hidden layer is the main difference in working between RBFNN and BPNN. Instead of the weighted sum of the input vector applied in BPNN, the distance between the input and the center is used in

the RBFNN training process [43]. Normally, Gaussian basis functions and linear transfer functions are used in the hidden layer and in the output layer, respectively. The Gaussian transfer function for the RBFN is shown in the following equation:

$$\phi_j(x) = \exp \left(-\frac{\|X - \mu_j\|^2}{2\sigma_j^2} \right) \quad (6)$$

where ϕ_j is the nonlinear function of unit j , x and μ are the input and the center of RBF unit, respectively. σ_j is the spread of the Gaussian basis function. The neurons of output layer lead to the weighted inputs and results are obtained through a linear combination, which is of a similar structure to that of the BPNN [46]:

$$\hat{y} = \sum_m^{i=1} w_i R_i(x) + b_2 \quad (7)$$

where \hat{y} is the RBFNN predicted result, b_2 is the bias in the output layer and w_i is the optimized connection weight obtained by using the learning process [44].

2.3. Fuzzy inference system and ANFIS models

Fuzzy modeling is the puissant method to catch relationship between input and output in nonlinear systems. Fuzzy modeling is one of the most powerful models to acquire relationship of input-output in complex nonlinear systems. Logical operation, membership function and if-then rules are deduced from fuzzy systems. Fig. 3 exhibits an FIS that contains fuzzy rules, fuzzifier, defuzzifier and fuzzy inference engine. In the fuzzy logic (FL) applications, the fuzzy rule (if-then rules) has played a central role. Fuzzy is linguistic variable which values are words rather than numbers. A fuzzy rule has the form, of if x is A then y is B , where A and B are linguistic values defined by fuzzy sets on universes of discourse X and Y , respectively. The fuzzy labels set are

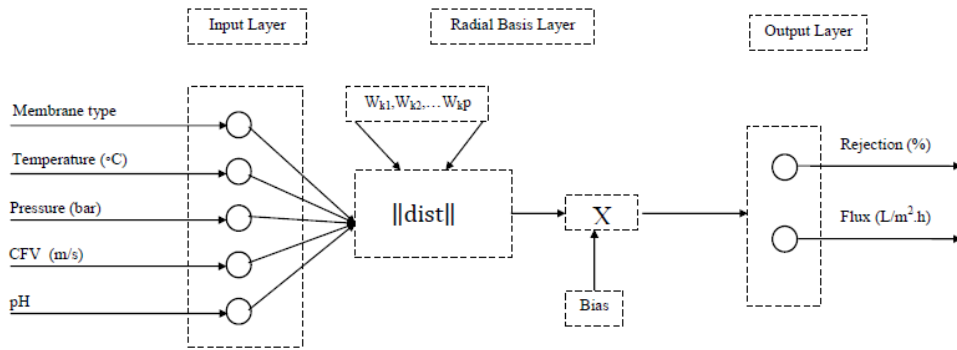


Fig. 2. An architecture of RBF model.

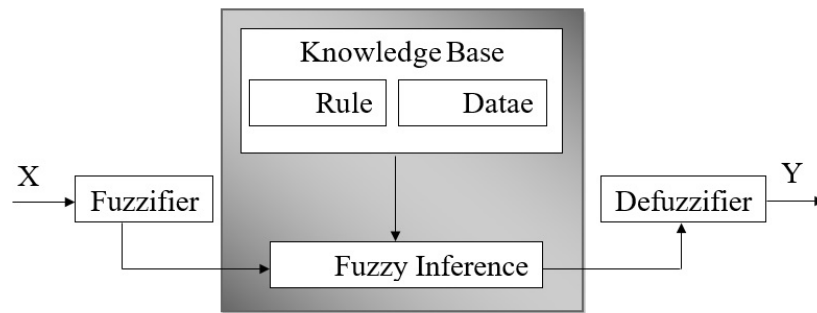


Fig. 3. A schematic of FIS.

demonstrated by database adequate membership functions. The premise or antecedent is the if-part of a fuzzy if-then rule, while the consequent or conclusion is the then-part of the rule. The fuzzy logic operators which consist of the fuzzy intersection or conjunction (AND), fuzzy complement (NOT) and fuzzy union or disjunction (OR) would resolve the antecedent to a single number between zero and 1, if there are multiple hypotheses [13]. Fuzzifier module converted the real numbers of input into fuzzy sets. The “If X” is the discourse universe and its elements are determined by x , then a fuzzy set A in X is indicated by a membership function $\mu_A(x)$ which takes values between 0 and 1. The Gaussian membership function as expressed in the following equation is obtained via various membership functions:

$$\mu_A(X) = e^{-\left(\frac{X-X^*}{\sigma}\right)^2} \quad (8)$$

where σ, x^* are parameters of function. The mean of defuzzification consists of centroid, bisector, smallest of maxima (SOM), largest of maxima (LOM) and the mean of maxima (MOM). The most typical defuzzifier designates the gravity center method in which the gravity center of the fuzzy set is calculated and projected to the x-axis to gain a non-fuzzy output real number region [47].

Fig. 4 displays the FIS structure. The Mamdani (Max-Min) [48] and Takagi-Sugeno model [49] are two common kinds of fuzzy inference systems. The consequences of the rules of Mamdani models are fuzzy sets, which include linguistic information into the model, while the output mem-

bership functions of the Takagi-Sugeno model is constant or linear functions.

Adaptive neuro-fuzzy inference system (ANFIS) is a combination of FIS and ANN. FIS and ANN are two supplementary methods. The incorporation of artificial neural network with learning ability and FIS with decision making ability can be used to construct a flexible intelligent system. Therefore, the combination of both artificial neural network and fuzzy inference system can improve system performance without interference of operators [50]. The advantage of this technique has led many researchers to apply the ANFIS architecture to model nonlinear functions to recognize nonlinear parameters as well as to forecast desired result logically [51]. The ANFIS structure shown in Fig. 5i indicates total layers of the system and the dependency of ANFIS rules on the variables.

2.4. Normalization of data

Normalization is an alteration process by which inputs and output vectors are scaled to a defined numerical range. Because of very small or very large data, normalization of data was used to avoid of numerical overfitting [20,38]. Therefore, data were scaled through the following equation:

$$X_{i,norm} = \frac{X - X_{min}}{X_{max} - X_{min}} \quad (9)$$

where $X_{i,norm}, X_{min}$ and X_{max} are the normalized, minimum and maximum values of X, respectively.

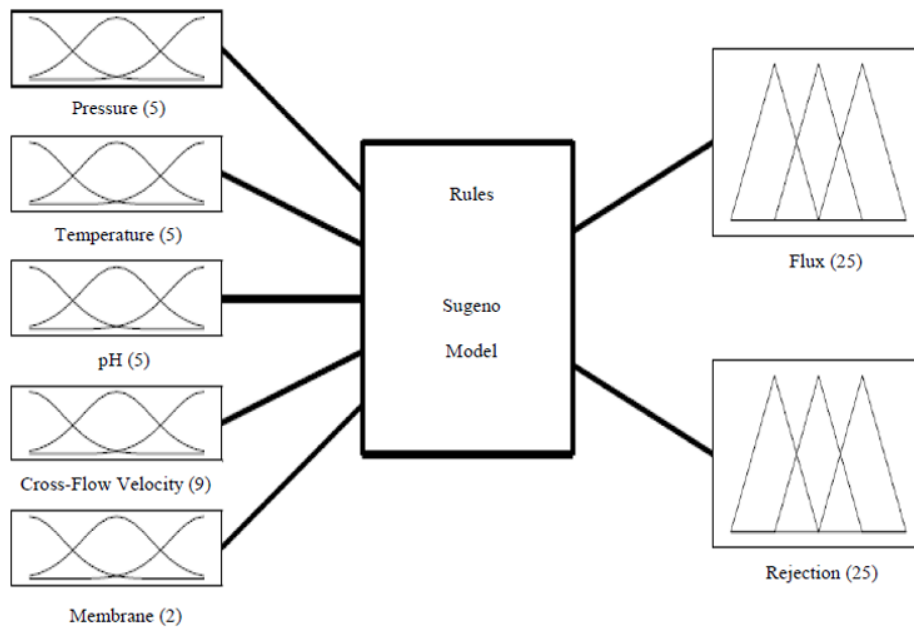


Fig. 4. An architecture of FIS model.

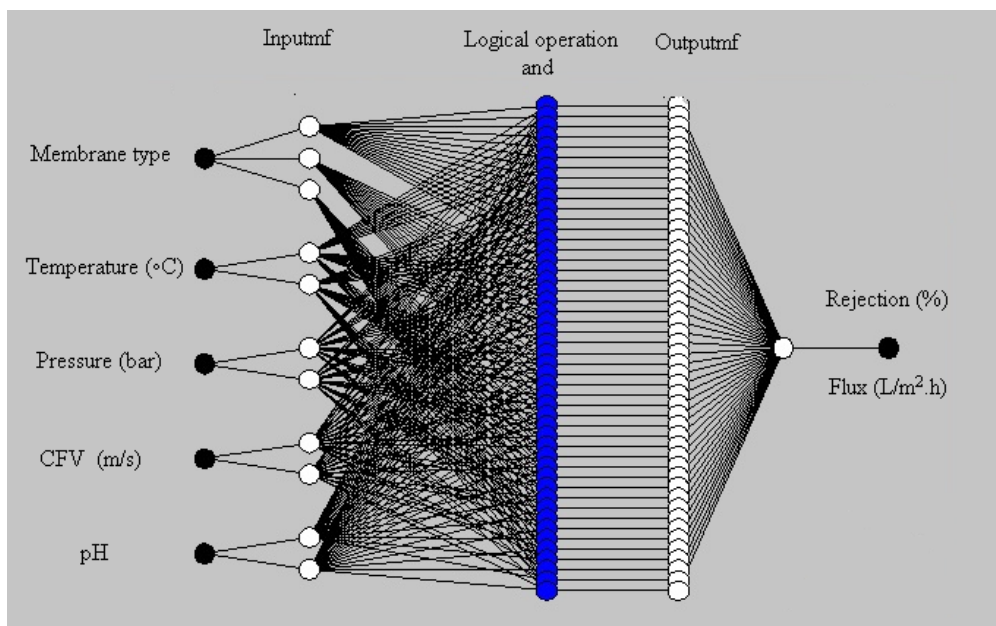


Fig. 5. The architecture of the ANFIS model.

2.5. Selection of optimal architecture

To obtain the optimum model, various structures were evaluated and the prediction performances of the various architectures were compared using the coefficient of determination (R^2) of the linear regression line between the predicted value and the desired output and the mean absolute error (MAE). The coefficient of determination and error functions are as follows:

$$MAE = \frac{1}{N} \sum_{i=1}^N (|y_{prd,i} - y_{exp,i}|) \quad (10)$$

$$R^2 = 1 - \frac{\sum_{i=1}^N (y_{prd,i} - y_{exp,i})^2}{\sum_{i=1}^N (y_{prd,i} - y_m)^2} \quad (11)$$

where $y_{prd,i}$, $y_{exp,i}$, N and y_m were the predicted value, the experimental value, the number of data and the average of the experimental value.

3. Results and discussion

The present research aimed to consider the ability of intelligent system models to forecast the permeate flux and rejection of membrane as a function of feed pH, membrane type (reverse osmosis and nanofiltration), transmembrane pressure, feed temperature and cross flow velocity. The results were divided into 3 parts. The results of RBF and BPNN models were elucidated in the first part. In the second part, the results of FIS model has been indicated. In the third part, the results of ANFIS model were demonstrated.

3.1. BPNN and RBF models

Fig. 6 shows the complexity of dependency on input/output data. Figs. 6A-B display input vectors and Figs. 6C-D indicate output vectors. The various structures of RBF and BPNN models have been used and their results are summarized in Table 1. It may be seen from Table 1 that the structure with 5 neurons gives simultaneously the best R^2 and MAE values for both training and testing sets. The existence of five inputs and two outputs make the training and prediction procedure very complicated. As indicated in Table 1, the coefficient of determination for training and testing data

set could not be better than 0.95 and 0.86, respectively. Fig. 7 displays the plot of the actual values of the normalized rejection and permeate flux of training and testing data sets against the values of normalized rejection and permeate flux predicted with a 5 hidden layers neurons structure. This indicates a good agreement between the simulated and the actual data. Fig. 8 demonstrates actual values of the normalized rejection and permeate flux against calculated values with best RBF model (spread constant of 10). The equation that achieved from the ANN model is considered as the objective function. This equation correlates the inputs with output and can be specified as follows:

$$\text{ANN output} = \text{Purelin}(w_2 * \text{tansig}(w_1 * [x(1); x(2); x(3); x(4); x(5)] + b_1) + b_2) \quad (12)$$

where $x(1)$, $x(2)$, $x(3)$, $x(4)$ and $x(5)$ show the inputs, w_1 and b_1 are the weight and bias of the hidden layer, while the w_2 and b_2 are the weight and bias of output layers. Table 2 presents the weight and bias values of each layer that determined from the optimum ANN structure.

3.2. FIS and ANFIS models

In this study, Sugeno model is used in FIS model. Fig. 9 shows a membership function (Gaussian) of input variable in the used model. For the input parameters nine membership functions VL, L, VMO, MO, M, I, VI, H, VH are

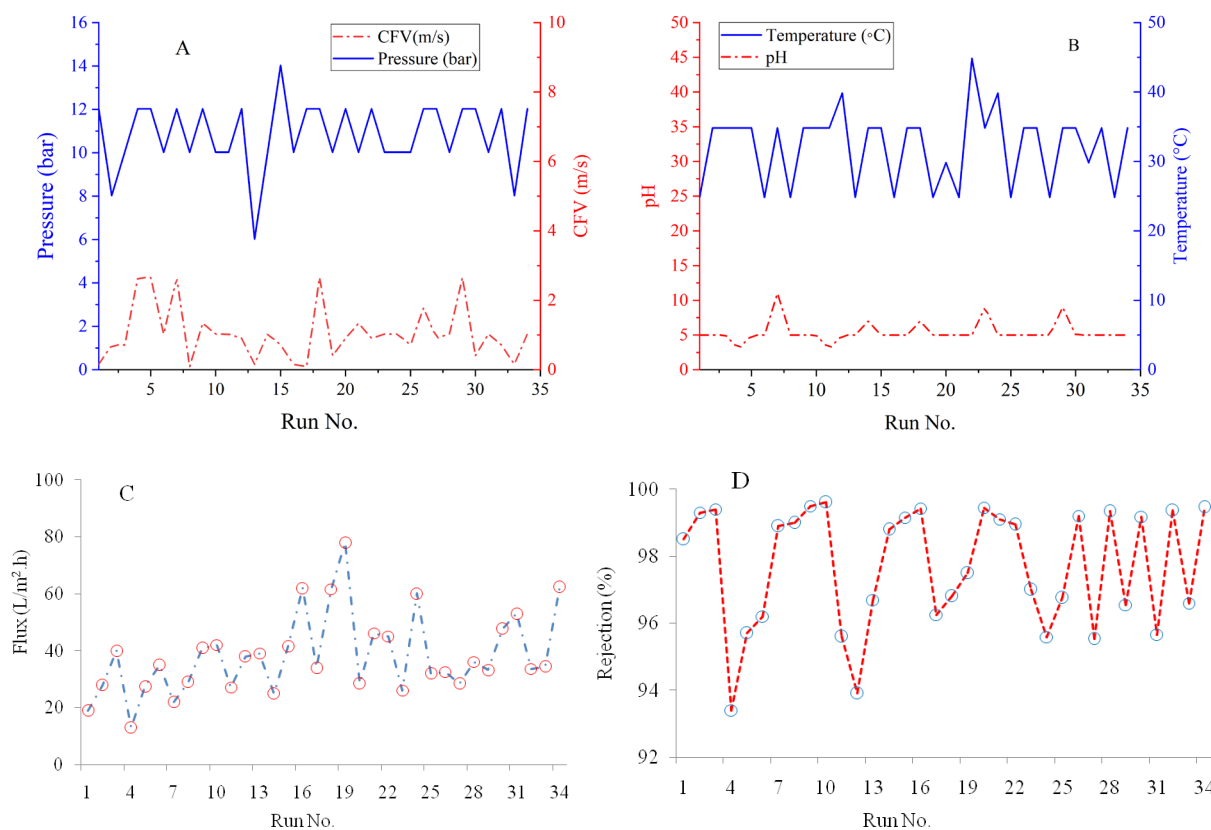


Fig. 6. The complexity of several experimental data relationships, (A)-(B) input dataset vectors, (C)-(D) output dataset vectors.

Table 1
The results of various structures of BPNN and RBF models

BPNN									
Hidden layer neurons	Flux (L/m ² ·h)				Rejection (%)				
	Training		Testing		Training		Testing		
	R ²	MAE	R ²	MAE	R ²	MAE	R ²	MAE	
2	0.86	0.004	0.87	0.006	0.60	0.70	0.52	0.098	
3	0.69	0.058	0.25	0.139	0.86	0.024	0.93	0.003	
4	0.20	0.289	0.62	0.231	0.63	0.062	0.82	0.031	
5	0.86	0.011	0.83	0.026	0.95	0.026	0.94	0.001	
6	0.32	0.155	0.36	0.135	0.70	0.104	0.77	0.054	
10	0.71	0.015	0.82	0.078	0.94	0.023	0.89	0.052	
15	0.79	0.047	0.66	0.063	0.76	0.042	0.99	0.033	
20	0.72	0.086	0.92	0.062	0.72	0.142	0.87	0.135	
2,1 (2 in 1st layer, 1 in 2nd layer)	0.63	0.378	0.33	0.105	0.77	0.680	0.93	0.015	
2,2 (2 in 1st layer, 2 in 2nd layer)	0.31	0.053	0.22	0.017	0.91	0.036	0.99	0.012	
3,2 (3 in 1st layer, 2 in 2nd layer)	0.33	0.112	0.71	0.024	0.60	0.054	0.93	0.081	
3,3 (3 in 1st layer, 3 in 2nd layer)	0.25	0.021	0.19	0.083	0.47	0.074	0.68	0.050	
4,3 (4 in 1st layer, 3 in 2nd layer)	0.21	0.081	0.22	0.057	0.22	0.105	0.67	0.023	
4,4 (4 in 1st layer, 4 in 2nd layer)	0.75	0.063	0.58	0.037	0.85	0.026	0.87	0.034	
5,4 (5 in 1st layer, 4 in 2nd layer)	0.19	0.035	0.23	0.030	0.71	0.040	0.97	0.020	
5,5 (5 in 1st layer, 5 in 2nd layer)	0.85	0.012	0.66	0.038	0.80	0.013	0.92	0.015	
10,5 (10 in 1st layer, 5 in 2nd layer)	0.67	0.058	0.37	0.120	0.95	0.014	0.82	0.081	
10,10 (10 in 1st layer, 10 in 2nd layer)	0.78	0.051	0.38	0.071	0.85	0.012	0.94	0.012	
15,10 (15 in 1st layer, 10 in 2nd layer)	0.55	0.021	0.62	0.022	0.71	0.019	0.93	0.013	
15,15 (15 in 1st layer, 15 in 2nd layer)	0.82	0.010	0.50	0.055	0.78	0.069	0.98	0.069	
20,15 (20 in 1st layer, 15 in 2nd layer)	0.33	0.042	0.74	0.030	0.94	0.017	0.94	0.018	
20,20 (20 in 1st layer, 20 in 2nd layer)	0.42	0.051	0.70	0.028	0.89	0.021	0.93	0.016	
RBF									
Spread constant									
1	1	1.3×10 ⁻⁵	0.23	0.874	1	3.1×10 ⁻¹²	0.46	0.113	
5	1	1.0×10 ⁻⁵	0.21	0.009	1	8.1×10 ⁻⁷	0.57	0.020	
10	0.99	2.0×10 ⁻⁵	0.60	0.001	1	1.5×10 ⁻⁶	0.78	0.042	

applied. They are very low, low, very moderate, moderate, medium, increase, very increase, high, very high, respectively. In this investigation, the fuzzy reasoning results of outputs are obtained by the aggregation operation of fuzzy sets of inputs and are designed fuzzy rules, where max aggregation method, the fuzzy implication operator defined by min and to gain a crisp output from the aggregation fuzzy result, whatever the defuzzification methods are utilized. Fig. 10 indicates the experimental data compared with the prediction of the permeate flux and rejection of the FIS model for training and testing data sets.

The accuracy and ability of a FIS tool for forecasting concentration licorice using RO and NF membrane performance was examined with experimental data shown in Table 2. It is found that the results from the presented FIS model are in agreement with experimental data.

As mentioned early, the ANFIS is a hybrid of neural network topology together with fuzzy logic, therefore, it is applied as a robust approach to simulate rejection and

permeate flux based on experimental results. In this study, two ANFIS models were built to simulate the rejection and permeate flux. The Sugeno type fuzzy inference system was used to achieve a concise model with a minimum number of rules. In both ANFIS models the inputs were the membrane type, pressure, temperature, pH and cross flow velocity, that Gaussian membership function with numbers of 2, 5, 5, 5, and 9, respectively was selected for these inputs by developing different models and taking into consideration the consequent parameters. The outputs of models were the permeate flux and rejection that constant type membership function was used for these outputs during generating FIS. The optimization methods train the membership function parameters to imitate the training data set.

In the optimum method, hybrid of back propagation was selected as the optimization method. The hybrid optimization method is a combination of least-squares and back-propagation gradient descent method. The hybrid method converges much faster since it diminishes the

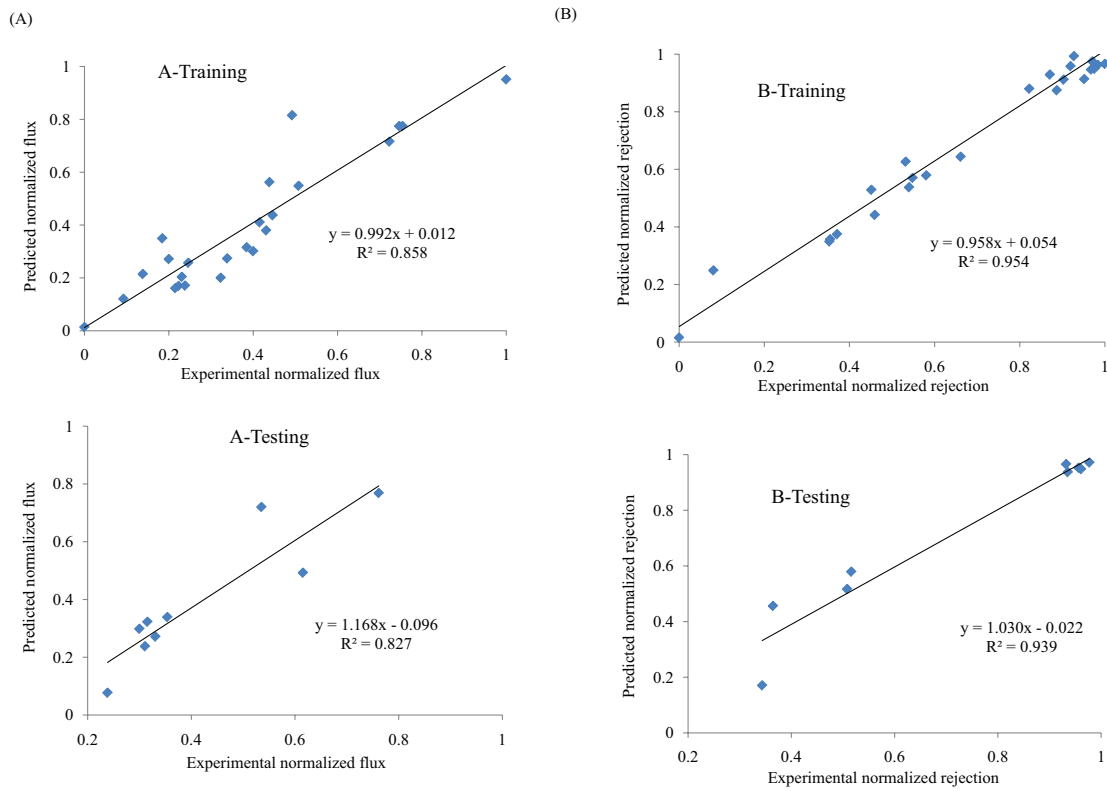


Fig. 7. Correlation between the normalized experimental values of training and testing data sets and the predicted values using BPNN model (A) permeate flux (B) rejection.

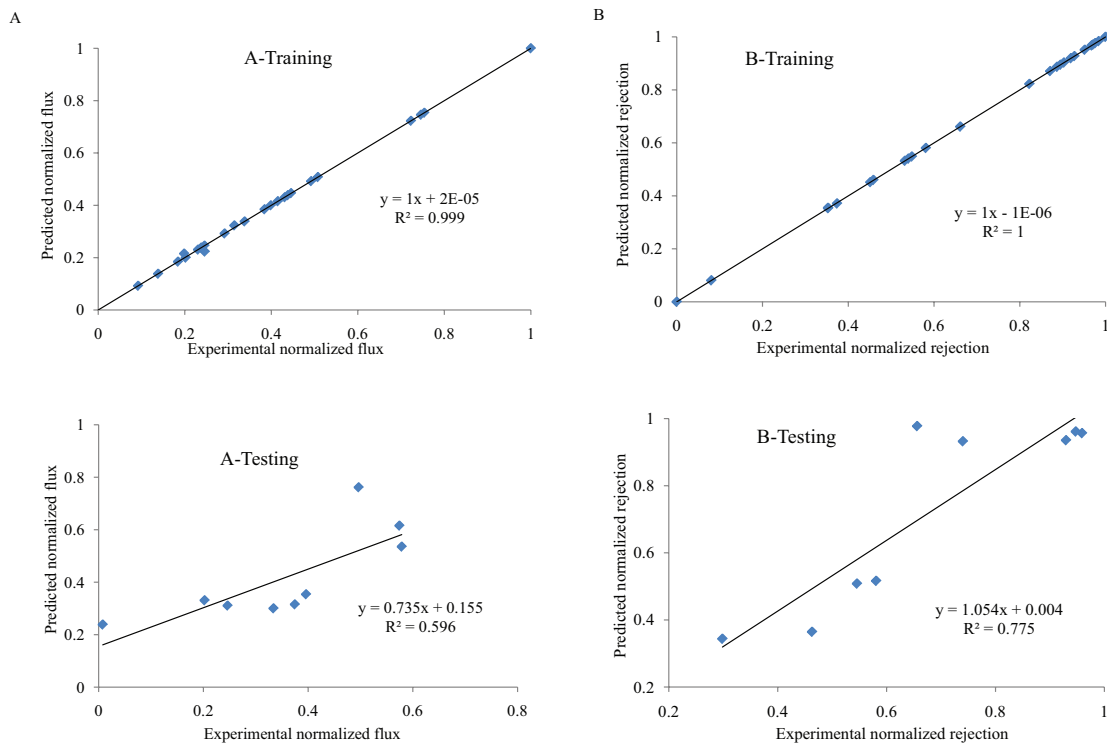


Fig. 8. Correlation between the normalized experimental values of training and testing data sets and the predicted values using the RBF model with a spread constant of 10 (A) permeate flux (B) rejection.

Table 2
The weight and bias of trained ANN model

W_1					W_2^T	b_1	b_2
-0.235	1.198	2.899	2.070	0.889	4.512	-0.133	-0.968
2.540	-0.841	2.141	-0.741	-1.284	0.601	0.1764	-0.227
0.575	-1.021	-0.364	-1.948	-0.229	2.986	-0.505	0.6749
-0.912	-4.261	-11.75	-6.410	4.248	0.5219	-0.209	3.603
-36.57	-15.96	0.360	63.378	3.213	0.1745	-0.055	-16.86

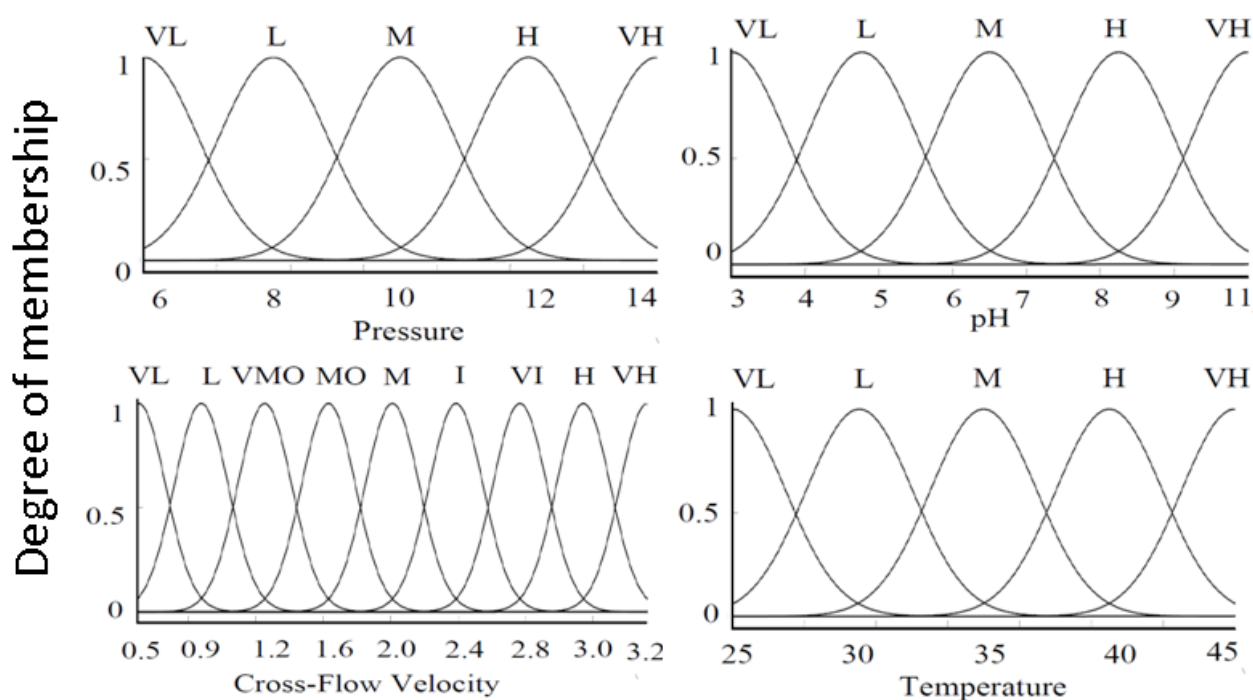


Fig. 9. Membership function of input variables used in this work (VL: very low, L: low, VMO: very moderate, MO: moderate, M: medium, I: increase, VI: very increase, H: high, VH: very high).

dimension of the search space of the original back-propagation approach. In this study, the hybrid optimization method, the epoch numbers of 100 and the error tolerance of training to adjust the stopping criteria for the training of 0 were used. A regression curve is plotted in Fig. 11 between the normalized experimental and predicted permeate flux and rejection via ANFIS model for training and testing sets. The R^2 and MAE of ANFIS model for training and testing sets are presented in Table 3. It can be seen that data are well fitted due to a high value of R^2 .

3.3. Comparison between models

BPNN, ANFIS, RBF and FIS models were selected to compare their abilities in predicting of the permeate flux and rejection obtained from experiments. Fig. 12 compares experimental results with RBF, BPNN, FIS and ANFIS forecasted values of testing data set using best models were selected. It was shown that the performance of ANFIS

model is better than other models and a good agreement between the experimental data and the predicted values using ANFIS was observed.

4. Conclusion

The main objective of this study was to construct and verify the capability of the models, namely BPNN, RBF, FIS and ANFIS to simulate and modeling of permeate flux and rejection in concentration processes using RO and NF membranes. The results revealed that there was a good agreement between the experimental data and the predicted data with the proposed model under different operating conditions. Therefore, it can be deduced that the ANFIS model can be applied as a feasible model to simulate the performance of the membranes under different operating conditions. By comparing the results obtained from the intelligent system, it can be concluded that the processes, namely concen-

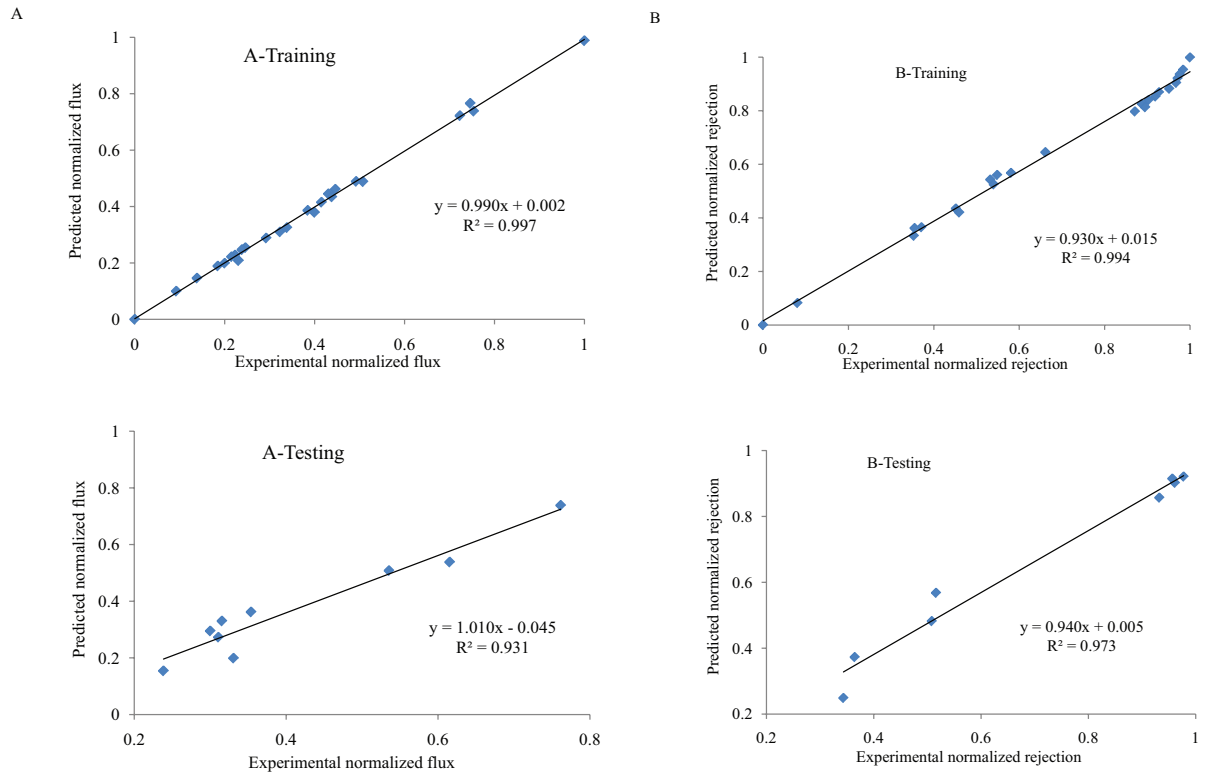


Fig. 10. Correlation between the normalized experimental values of training and testing data sets and the predicted values using FIS model (A) permeate flux (B) rejection.

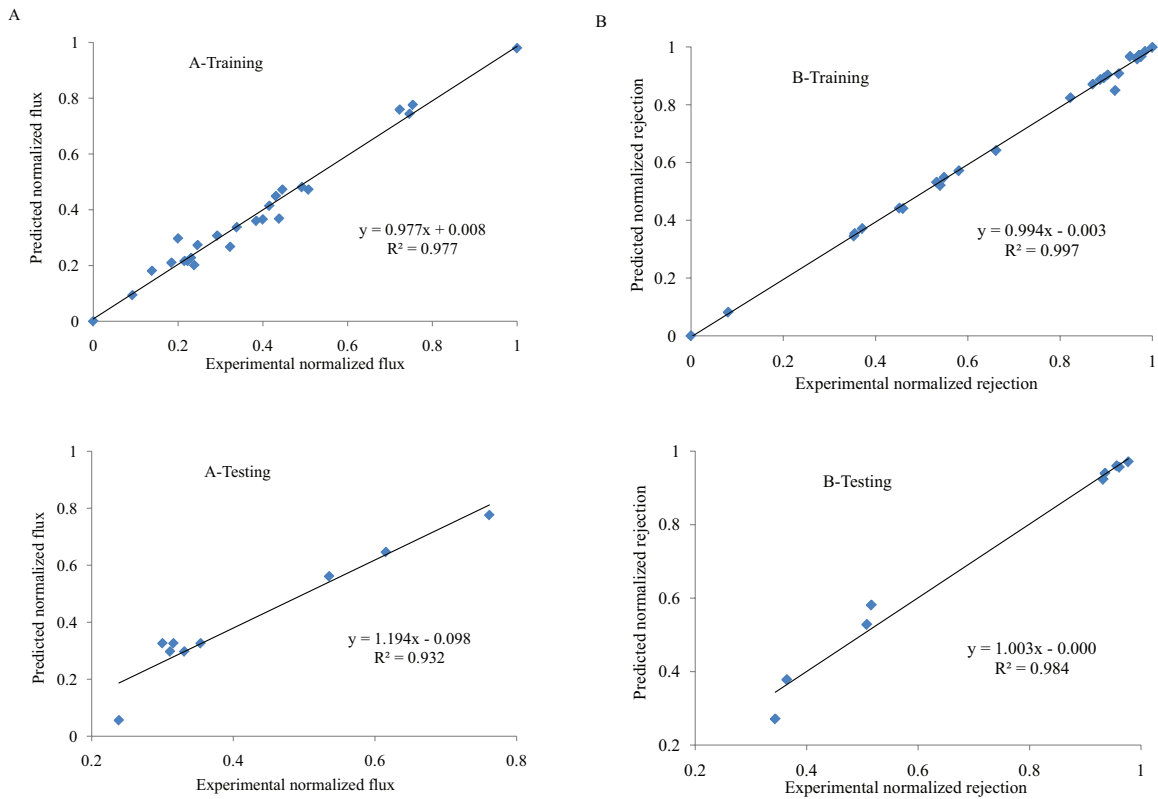


Fig. 11. Correlation between the normalized experimental values of training and testing data sets and the predicted values using ANFIS model (A) permeate flux (B) rejection.

Table 3
R² and MAE of FIS and ANFIS models for training and testing data sets

Model	Flux (L/m ² ·h)				Rejection (%)			
	Training		Testing		Training		Testing	
	R ²	MAE	R ²	MAE	R ²	MAE	R ²	MAE
FIS	0.997	0.002	0.931	0.041	0.994	0.032	0.975	0.039
ANFIS	0.997	0.0001	0.932	0.017	0.997	0.007	0.984	0.001

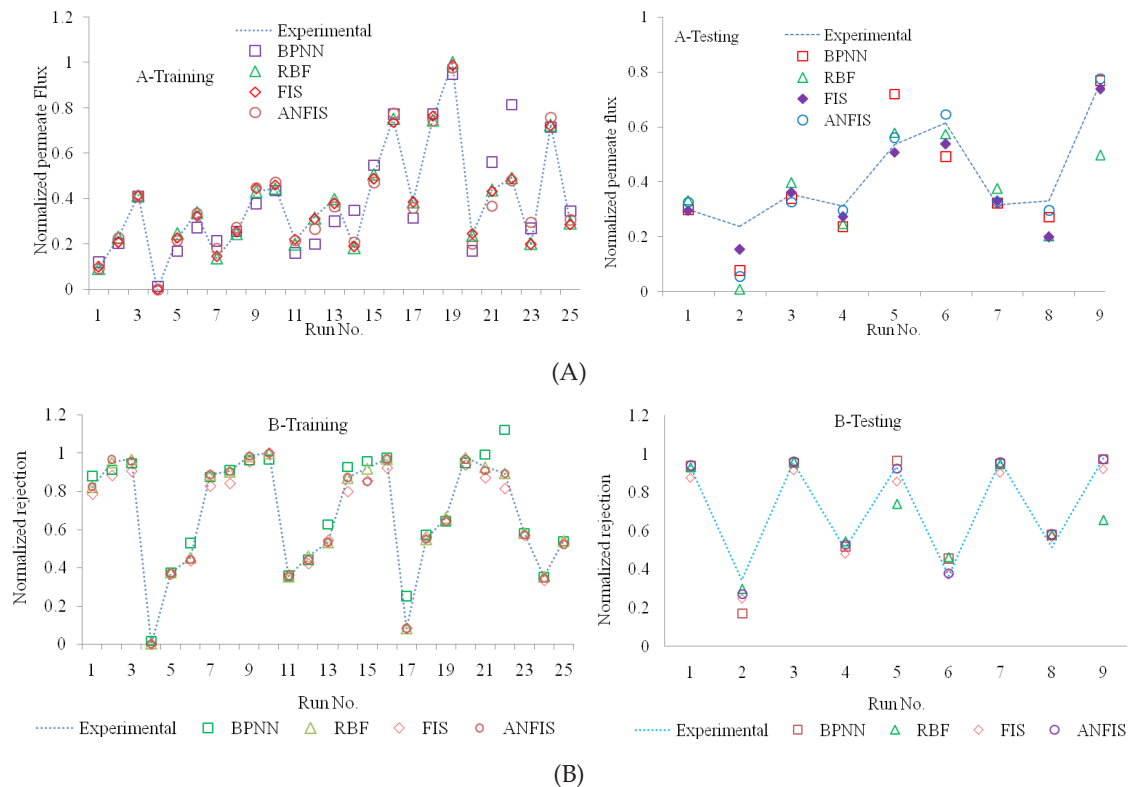


Fig. 12. Correlation between the normalized experimental values of training and testing data sets and the predicted values using ANFIS model (A) permeate flux (B) rejection.

tration with different and effective parameters, will tempt us to use the ANFIS systems instead of the trial and error method, which is both time and cost consuming.

References

- [1] T.Y. Wong, S.-m. Lin, C.H. Poon, L.K. Leung, The licorice flavonoid isoliquiritigenin reduces DNA-binding activity of AhR in MCF-7 cells, *Chem. Biol. Interact.*, 221 (2014) 70–76.
- [2] M. Bahmani, M. Rafeian-Kopaei, M. Jeloudari, Z. Eftekhari, B. Delfan, A. Zargar, S. Forouzan, A review of the health effects and uses of drugs of plant licorice (*Glycyrrhiza glabra* L.) in Iran, *Asian Pac. J. Trop. Dis.*, 4(S2) (2014) S847–S849.
- [3] R. Yang, L.-q. Wang, Y. Liu, Antitumor activities of widely-used Chinese herb—licorice, *Chin. Herbal Med.*, 6 (2014) 274–281.
- [4] E.A. Al-Dujaili, C. Kenyon, M. Nicol, J. Mason, Licorice and glycyrrhetic acid increase DHEA and deoxycorticosterone levels in vivo and invitro by inhibiting adrenal SULT2A1 activity, *Mol. Cell. Endocrinol.*, 336 (2011) 102–109.
- [5] S.-J. Ahn, Y.-D. Song, S.-J. Mah, E.-J. Cho, J.-K. Kook, Determination of optimal concentration of deglycyrrhized licorice root extract for preventing dental caries using a bacterial model system, *J. Dent. Sci.*, 9 (2014) 214–220.
- [6] M. Al-Obaidi, C. Kara-Zaitri, I.M. Mujtaba, Development of a mathematical model for apple juice compounds rejection in a spiral-wound reverse osmosis process, *J. Food Eng.*, 192 (2017) 111–121.
- [7] Z. Jin, H. Gong, K. Wang, Application of hybrid coagulation microfiltration with air backflushing to direct sewage concentration for organic matter recovery, *J. Hazard. Mater.*, 283 (2015) 824–831.
- [8] C. Zambra, J. Romero, L. Pino, A. Saavedra, J. Sanchez, Concentration of cranberry juice by osmotic distillation process, *J. Food Eng.*, 144 (2015) 58–65.
- [9] Y. Wang, B. Shi, Concentration of gelatin solution with polyethersulfone ultrafiltration membranes, *Food Bioprod. Process.*, 89 (2011) 163–169.
- [10] M.R. Sohrabi, S.S. Madaeni, M. Khosravi, A.M. Ghaedi, Concentration of licorice aqueous solutions using nanofiltration and reverse osmosis membranes, *Sep. Purif. Technol.*, 75 (2010) 121–126.

- [11] M. Al-Obaidi, C. Kara-Zaitri, I.M. Mujtaba, Optimum design of a multi-stage reverse osmosis process for the production of highly concentrated apple juice, *J. Food Eng.*, 214 (2017) 47–59.
- [12] G. Rajauria, B.K. Tiwari, *Fruit Juices: Extraction, Composition, Quality and Analysis*, Academic Press, 2017.
- [13] S.S. Madaeni, A.R. Kurdian, Fuzzy modeling and hybrid genetic algorithm optimization of virus removal from water using microfiltration membrane, *Chem. Eng. Res. Des.*, 89 (2011) 456–470.
- [14] B.K. Nandi, A. Moparthy, R. Uppaluri, M.K. Purkait, Treatment of oily wastewater using low cost ceramic membrane: Comparative assessment of pore blocking and artificial neural network models, *Chem. Eng. Res. Des.*, 88 (2010) 881–892.
- [15] M.A. Al-Obaidi, C. Kara-Zaitri, I.M. Mujtaba, Wastewater treatment by spiral wound reverse osmosis: Development and validation of a two dimensional process model, *J. Clean. Prod.*, 140 (2017) 1429–1443.
- [16] M.A. Al-Obaidi, C. Kara-Zaitri, I.M. Mujtaba, Optimum design of a multi-stage reverse osmosis process for the production of highly concentrated apple juice, *J. Food Eng.*, 214 (2017) 47–59.
- [17] M.A. Al-Obaidi, I.M. Mujtaba, Steady state and dynamic modeling of spiral wound wastewater reverse osmosis process, *Comput. Chem. Eng.*, 90 (2016) 278–299.
- [18] S. Curcio, V. Calabrò, G. Iorio, A theoretical analysis of transport phenomena in membrane concentration of liquorice solutions: a FEM approach, *J. Food Eng.*, 71 (2005) 252–264.
- [19] Y. Vural, D.B. Ingham, M. Pourkashanian, Performance prediction of a proton exchange membrane fuel cell using the ANFIS model, *Int. J. Hydrogen Energy*, 34 (2009) 9181–9187.
- [20] P. Rai, G. Majumdar, S. DasGupta, S. De, Modeling the performance of batch ultrafiltration of synthetic fruit juice and mosambi juice using artificial neural network, *J. Food Eng.*, 71 (2005) 273–281.
- [21] A. Castro, R. Carballo, G. Iglesias, J. Rabuñal, Performance of artificial neural networks in nearshore wave power prediction, *Appl. Soft Comput.*, 23 (2014) 194–201.
- [22] M. Pérez-Godoy, A.J. Rivera, C. Carmona, M. del Jesus, Training algorithms for radial basis function networks to tackle learning processes with imbalanced data-sets, *Appl. Soft Comput.*, 25 (2014) 26–39.
- [23] B. Kaushik, H. Banka, Performance evaluation of approximated artificial neural network (AANN) algorithm for reliability improvement, *Appl. Soft Comput.*, 26 (2014) 303–314.
- [24] A. Tardast, M. Rahimnejad, G. Najafpour, A. Ghoreyshi, G.C. Premier, G. Bakeri, S.-E. Oh, Use of artificial neural network for the prediction of bioelectricity production in a membrane less microbial fuel cell, *Fuel*, 117 (2014) 697–703.
- [25] A. Maghsoodi, E. Afshari, H. Ahmadikia, Optimization of geometric parameters for design a high-performance ejector in the proton exchange membrane fuel cell system using artificial neural network and genetic algorithm, *Appl. Therm. Eng.*, 71 (2014) 410–418.
- [26] H. Nourbakhsh, Z. Emam-Djomeh, M. Omid, H. Mirsaeeedghazi, S. Moini, Prediction of red plum juice permeate flux during membrane processing with ANN optimized using RSM, *Comput. Electron. Agric.*, 102 (2014) 1–9.
- [27] C. Aydiner, I. Demir, E. Yildiz, Modeling of flux decline in crossflow microfiltration using neural networks: the case of phosphate removal, *J. Membr. Sci.*, 248 (2005) 53–62.
- [28] V. Yangali-Quintanilla, A. Verliefe, T.U. Kim, A. Sadmani, M. Kennedy, G. Amy, Artificial neural network models based on QSAR for predicting rejection of neutral organic compounds by polyamide nanofiltration and reverse osmosis membranes, *J. Membr. Sci.*, 342 (2009) 251–262.
- [29] S. Chellam, Artificial neural network model for transient cross-flow microfiltration of polydispersed suspensions, *J. Membr. Sci.*, 258 (2005) 35–42.
- [30] Y.G. Lee, Y.S. Lee, J.J. Jeon, S. Lee, D.R. Yang, I.S. Kim, J.H. Kim, Artificial neural network model for optimizing operation of a seawater reverse osmosis desalination plant, *Desalination*, 247 (2009) 180–189.
- [31] G.R. Shetty, S. Chellam, Predicting membrane fouling during municipal drinking water nanofiltration using artificial neural networks, *J. Membr. Sci.*, 217 (2003) 69–86.
- [32] M. Sadrzadeh, T. Mohammadi, J. Ivakpour, N. Kasiri, Separation of lead ions from wastewater using electro dialysis: Comparing mathematical and neural network modeling, *Chem. Eng. J.*, 144 (2008) 431–441.
- [33] Q.-F. Liu, S.-H. Kim, S. Lee, Prediction of microfiltration membrane fouling using artificial neural network models, *Sep. Purif. Technol.*, 70 (2009) 96–102.
- [34] A. Ghaedi, A. Vafaei, M. Mohagheghian, N. Afshar, S. Hafezi, Fuzzy modelling of concentration in chamomile solution using reverse osmosis, *Fresenius Environ. Bull.*, 21 (2012) 634–643.
- [35] B. Rahmanian, M. Pakizeh, M. Esfandyari, F. Heshmatnezhad, A. Maskooki, Fuzzy modeling and simulation for lead removal using micellar-enhanced ultrafiltration (MEUF), *J. Hazard. Mater.*, 192 (2011) 585–592.
- [36] G. Özkan, M. Inal, Comparison of neural network application for fuzzy and ANFIS approaches for multi-criteria decision making problems, *Appl. Soft Comput.*, 24 (2014) 232–238.
- [37] A. Abdulshahed, A.P. Longstaff, S. Fletcher, A. Myers, Comparative study of ANN and ANFIS prediction models for thermal error compensation on CNC machine tools, in: *Lamdamap 10th International Conference, EUSPEN*, 2013.
- [38] J. Sargolzaei, M. Haghighi Asl, A. Hedayati Moghaddam, Membrane permeate flux and rejection factor prediction using intelligent systems, *Desalination*, 284 (2012) 92–99.
- [39] S. Azadi, A. Karimi-Jashni, S. Javadpour, Modeling and optimization of photocatalytic treatment of landfill leachate using tungsten-doped TiO₂ nano-photocatalysts: Application of artificial neural network and genetic algorithm, *Process Saf. Environ. Prot.*, 117 (2018) 267–277.
- [40] Z.C. Lipton, J. Berkowitz, C. Elkan, A critical review of recurrent neural networks for sequence learning, *arXiv preprint arXiv:1506.00019*, (2015).
- [41] S. Xu, L. Chen, A novel approach for determining the optimal number of hidden layer neurons for FNN's and its application in data mining, in: *5th International Conference on Information Technology and Applications (ICITA 2008)*, Cairns, Queensland, Australia, 2008.
- [42] G. Panchal, M. Panchal, Review on methods of selecting number of hidden nodes in artificial neural network, *Int. J. Comput. Sci. Mobile Comput.*, 3 (2014) 455–464.
- [43] H. Chen, A.S. Kim, Prediction of permeate flux decline in crossflow membrane filtration of colloidal suspension: a radial basis function neural network approach, *Desalination*, 192 (2006) 415–428.
- [44] I. Yilmaz, O. Kaynar, Multiple regression, ANN (RBF, MLP) and ANFIS models for prediction of swell potential of clayey soils, *Expert Syst. Appl.*, 38 (2011) 5958–5966.
- [45] A. Shahsavand, F. Derakhshan Fard, F. Sotoudeh, Application of artificial neural networks for simulation of experimental CO₂ absorption data in a packed column, *J. Nat. Gas Sci. Eng.*, 3 (2011) 518–529.
- [46] T.A. Awchi, Application of radial basis function neural networks for reference evapotranspiration prediction, *AI-Rafi-dain Eng.*, 16 (2008) 117–129.
- [47] J. Sargolzaei, M. Khoshnoodi, N. Saghatoleslami, M. Mousavi, Fuzzy inference system to modeling of crossflow milk ultrafiltration, *Appl. Soft Comput.*, 8 (2008) 456–465.
- [48] Mamdani, Application of fuzzy logic to approximate reasoning using linguistic synthesis, *IEEE Trans. Comput.*, C-26 (1977) 1182–1191.
- [49] T. Takagi, M. Sugeno, Fuzzy identification of systems and its applications to modeling and control, *IEEE Trans. Syst. Man Cybern.*, (1985) 116–132.
- [50] M. Sahu, P. Singh, S.S. Mahapatra, K.K. Khatua, Prediction of entrance length for low Reynolds number flow in pipe using neuro-fuzzy inference system, *Expert Syst. Appl.*, 39 (2012) 4545–4557.
- [51] C. Carnevale, G. Finzi, E. Pisoni, M. Volta, Neuro-fuzzy and neural network systems for air quality control, *Atmos. Environ.*, 43 (2009) 4811–4821.